Physica Scripta. Vol. 31, 419–426, 1985

Measurement of Single Molecule Cross-Correlation Functions Using Electric Field Induced Birefringence

M. W. Evans

Department of Physics, U.C.N.W., Bangor, Gwynedd, United Kingdom

Received June 6, 1984; accepted January 12, 1985

Abstract

A method is derived for the measurement of the single molecule cross-correlation function $\langle \mathbf{v}(t)\boldsymbol{\omega}^{\mathrm{T}}(0)\rangle$ in the laboratory frame of reference. This consists of measuring the angular velocity a.c.f.'s in the x and z directions of the laboratory frame after inducing birefringence in the molecular liquid with an electric field E in the z axis. The cross-correlation function is then a convolution of the two angular velocity a.c.f.'s and the Fourier transform of the c.c.f. is, approximately, a ratio of the far infra-red spectra in the x and z axes.

The time dependence of $\langle \mathbf{v}(t)\boldsymbol{\omega}^{\mathrm{T}}(0)\rangle$ is analysed using computer simulation and simplified analytical theory for different electric field strengths E. (Here v is the molecular centre of mass *linear* velocity and $\boldsymbol{\omega}$ the molecular velocity).

1. Introduction

The classical theory of molecular diffusion originates with Einstein and later with Debye, who developed a model for the evolution of the molecular trajectory with time. Each molecular dipole was fixed in a rigid sphere, which was assumed to rotate in space, to be subjected to random white noise coupled about its axis of rotation, and to the action of an electric field in an axis of the laboratory frame. The classical theory is, therefore, based on a Smoluchowski equation of the type [1]:

$$\frac{\partial f}{\partial t}(\theta, t) = \frac{1}{\sin\theta}\frac{\partial}{\partial\theta} \times \left[\sin\theta\left(\frac{kT}{\zeta}\frac{\partial f}{\partial\theta}(\theta, t) + \frac{\mu E}{\zeta}\sin\theta\, f(\theta, t)\right)\right] \tag{1}$$

For the purposes of this paper it is important to note the presence of the electric field interaction term on the right hand side of eqn. (1). In the eqn. (1) $f\mathrm{d}\Omega$ is the number of dipoles whose axes point into an element of solid angle $\mathrm{d}\Omega$. The distribution function f is, therefore, a function of time t, and of the angle θ between the dipole axis and the applied field. The average torque on an individual dipole due to its surroundings is $\zeta\dot{\theta}$. Eqn. (1) is also the starting point for theories of electric field-induced birefringence, (Kerr effect) and provides the transient orientational average

$$\langle\cos\theta(t)\rangle = \frac{\mu E_0}{3kT}e^{-t/\tau} \tag{2}$$

after the electric field is switched off instantaneously at $t = 0$.

In spectroscopic measurements of molecular diffusion [2] the sample, e.g. a molecular liquid, is perturbed with an external field – an electromagnetic, magnetic, electric or mechanical (shearing) field. An electric field produces a torque on each molecule of $-\boldsymbol{\mu}\times\mathbf{E}$ which tilts them on average in the direction of E in the lab. frame. This polarises the sample slightly, and this polarisation is picked up as a change in capacitance and conductance on sensitive bridges; the well-known technique of dielectric spectroscopy. In infra-red spectroscopy the sample absorbs electromagnetic radiation, the power absorption ($\alpha(\bar{\nu})$) being related to the dielectric loss (ϵ'') through Maxwell's equations, viz.

$$\alpha(\bar{\nu}) = [2\pi\bar{\nu}\epsilon''(\bar{\nu})]/n(\bar{\nu})$$

$$n(\bar{\nu}) = [\tfrac{1}{2}(\epsilon''(\bar{\nu})^2 + \epsilon'(\bar{\nu})^2)^{1/2} + \epsilon'(\bar{\nu})]^{1/2} \tag{3}$$

Here $n(\bar{\nu})$ is the refractive index, $\epsilon'(\bar{\nu})$ the permittivity, $\bar{\nu}$ the wavenumber (in cm^{-1}) and $\alpha(\bar{\nu})$ the infra-red power absorption coefficient in neper cm^{-1}.

Therefore, the spectroscopy of molecular diffusion *never* reports the molecular ensemble free of external perturbation. (It is worth risking another truism here to point out that the relations (3) imply the presence of an external field in the sample.) Information about the isolated, unperturbed, sample is *interpolated* from the fluctuation-dissipation theorem. This theorem implies that the fall transient (eqn. (2)) and the orientational auto-correlation function $\langle\cos\theta(t)\cos\theta(0)\rangle$ of the *isolated* sample have the same time-dependence.

Recent electric-field-effect computer simulations have shown [3] that this is not even approximately true when the interaction energy per molecule, $\mu E\cos\theta$, is of the same order of magnitude as the thermal energy per molecule (kT). In general, the fluctuation-dissipation equality is only approximately true even in the linear response region of the Langevin function: $\mu E \ll kT$. What is happening in conventional spectroscopy is that the probe field is picking up a "signal" which is in general much weaker than the thermal "noise". Debye's was the first attempt at investigating the nature of this signal, generated by the field perturbation term on the right hand side of eqn. (1).

It is known now that this equation leaves out of consideration numerous features. The inertial term is missing and there is no attempt to represent the potential energy between the diffusing molecule and its neighbours, and there is no specific consideration of single molecule cross-correlations. We show in this paper that the cross-correlation function (c.c.f.) $\mathbf{C}_{\mathrm{tr}} = \langle \mathbf{v}(t)\boldsymbol{\omega}^{\mathrm{T}}(0)\rangle$ *becomes visible in the laboratory frame* whenever a molecular ensemble is perturbed by an external force field, specifically an electric field, so that $\langle\cos\theta(t)\rangle$ of eqn. (2) is finite. *It is precisely this perturbation* which allows us to see spectra, specifically dielectric spectra (permittivity dispersion and loss). In molecular dynamical terms the difference between a perturbed and isolated sample is that in the former case $\mathbf{C}_{\mathrm{tr}}$ *exists* and in the latter $\mathbf{C}_{\mathrm{tr}} = 0$ *for all* t because the parity of v is opposite to $\boldsymbol{\omega}$.

The approximations inherent in linear response theory now become apparent. *During the fall transient process* (eqn. (2)) a

transition in the dynamics is taking place whereby $C_{tr} \neq 0$ (field-on) $\rightarrow C_{tr} = 0$ (field-off). At field-off equilibrium, on the other hand, C_{tr} always vanishes, so that the time-dependence of the orientational fall-transient and the field-off equilibrium orientational a.c.f. *cannot be the same.* In other words, the *spectroscopy of molecular diffusion always picks up information on c.c.f.'s such as* C_{tr}. (A referee has made the very interesting remark in this context that the cross-correlation function C_{tr} *has no meaning in linear response theory.* There is no term corresponding to it in Onsager's thermodynamics and reciprocal relations. Therefore it follows that linear response theory, of which the fluctuation-dissipation theorem is a part, *is only an approximation to the true situation even when the transport properties of the system appear to be linear.*)

This has been "half-realised" in the literature, but not worked out quantitatively. Amost exactly 50 years after Debye's paper Condiff and Dahler [4] proposed a theory for C_{tr} based partly on an extension of the Langevin equation for rototranslation. These authors pointed out that several phenomena of fluid dynamics are based on C_{tr} and are known experimentally to be stimulated by the interaction of radiation fields with molecular multipoles. Since then the theoretical investigation of C_{tr} with Fokker-Planck and Langevin equations has accelerated. However, the tremendous complexity of these theories often obscures the results, and there is in consequence little attempt at experimental comparison. Steiger and Fox [5] recently claim to have found inconsistencies in some earlier treatments in the literature. These theories must satisfy the field-off parity theorem $C_{tr} = 0$ described by Berne and Pecora [6] when dealing with the single molecule c.c.f. It is not always clear that they do so.

The subject has received a new impetus recently through the use of computer simulation, Ryckaert et al. [7], were the first to point out that the field-off c.c.f. matrix:

$$C_{tr}^{(m)} = \langle \mathbf{v}(t)\boldsymbol{\omega}^{T}(0)\rangle_{(m)}$$

exists for $t > 0$ in a molecule fixed frame of reference, specifically that of the principal molecular moments of inertia. Their work for linear symmetry has been extended to C_{3v}, C_{2v}, C_1 and chiral symmetries by Evans and co-workers [8–15]. An interesting spin-off from this computer simulation work is the explanation [16, 17] of the physical differences between an enantiomer and racemic mixture in terms of two elements of $C_{tr}^{(m)}$ which mirror each other in both cases for R and S enantiomer but vanish for all t in the racemic mixture. There are no definite indications as yet from computer simulation that C_{tr} exists, even for chiral symmetry [17], in the absence of a probe field. For chiral symmetry (i.e. no symmetry) the complicated Langevin and Fokker-Planck equations are useless in this context, except as first approximations, because of the large number of phenomenological parameters needed.

In this paper we take a simple 3 x 3 site-site model of the CH_2Cl_2 intermolecular pair potential and use the technique of field-effect computer simulation to look for C_{tr} in the molecular liquid at 296 K. This has been found and characterised in this work with a static electric field **E** in the z axis of the laboratory frame. The dependence of C_{tr} may be characterised for very weak probe fields, $\mu E \ll kT$ by using the well-known technique of "non-equilibrium" molecular dynamics simulation [18]. The signal (C_{tr}) may be picked up from the thermal noise by comparing directly two runs, one with and the other without the application of an electric field.

2. Algorithm and Computer Simulation Method

The original listing TR12 of Singer et al. was modified by Ferrario and Evans [8, 9] to include partial charge terms on each site and was used as described elsewhere to develop the technique of field-effect computer simulation. The effect of an external electric field is simulated with an extra torque term $-\boldsymbol{\mu} \times \mathbf{E}$ in the forces loop of the algorithm, which may then be used to look at rise transients, field-on equilibrium correlation functions, and fall transients. The technique has been used already [19] to verify the field-on decoupling effect produced theoretically [20] by Grigolini and to verify the field-dependent nature of rise-transients, predicted from eqn. (1) by Morita [21] and Coffey et al. [22]. Perhaps the most important discovery of this method is that of fall-transient acceleration [23]. The fall transients from a birefringent molecular liquid fall more quickly than the equivalent equilibrium a.c.f., and are accelerated considerably with increasing field strength **E**. This is, of course, a violation of the fluctuation-dissipation theorem. Eqn. (1) and all single "particle" linear diffusion equations of this type do not produce fall-transient acceleration, i.e. the fall-transient and equilibrium a.c.f. are identical, *even when* $E \rightarrow \infty$. Fall transient acceleration has been used by Grigolini and co-workers [19] as evidence for the non-linear nature of the molecular liquid state at equilibrium i.e. the details of the intermolecular pair potential have to be known for a proper description, both at field-off *and* field-on equilibrium. It is clear now that fall-transient acceleration is also tied up with the process C_{tr} (field-on) $\rightarrow C_{tr}$ (field-off) $= 0$.

The intermolecular pair potential used in this paper is a 3 x 3 site-site model with Lennard-Jones atom-atom potential terms and partial charges to represent the electrostatic interaction: $\epsilon/k(\text{Cl–Cl}) = 173.5$ K; $\epsilon/k(\text{CH}_2\text{–CH}_2) = 70.5$ K; $\sigma(\text{CH}_2\text{–CH}_2) = 3.96$ A; $\sigma(\text{Cl–Cl}) = 3.35$ A; $q_{\text{Cl}} = -0.15|e|$; $q_{\text{CH}_2} = 0.30|e|$. The cross-correlation functions are evaluated with running time averaging and are normalised, as for example:

$$C_{tr}^{xy} = \langle v_x(t)\omega_y(0)\rangle / (\langle v_x^2\rangle^{1/2}\langle \omega_y^2\rangle^{1/2})$$

The noise level in the simulation is estimated as the difference between two successive runs. By symmetry, C_{tr} vanishes at $t = 0$, providing another estimate of the noise level. Approximately 1000 records (3000 time steps each of 5×10^{-15} s) were used in constructing C_{tr} elements. The statistics of the simulation could be improved considerably by longer runs, or by implementing "non-equilibrium" computer simulation methods.

3. Results and Discussion

The application of an electric field produces orientational rise transients. The 1/e level of each transient is a rise transient-time (RTT). These are field-strength dependent [3]. The $t \rightarrow \infty$ level of each transient falls on a first-order Langevin function of $\mu E/kT$. This is a check on the validity of the technique at field-on equilibrium.

The prime result of this paper is illustrated in Figs. (1) as a function of field strength. These figures illustrate the appearance of C_{tr} in the laboratory frame in terms of the dominant elements C_{tr}^{xy} and C_{tr}^{yx}. By "dominant elements" we mean that their normalised amplitudes, (the maximum of the first peak), are much bigger than the equivalent amplitudes of the other off-diagonal c.c.f.:s of C_{tr}. We have looked for these elements but

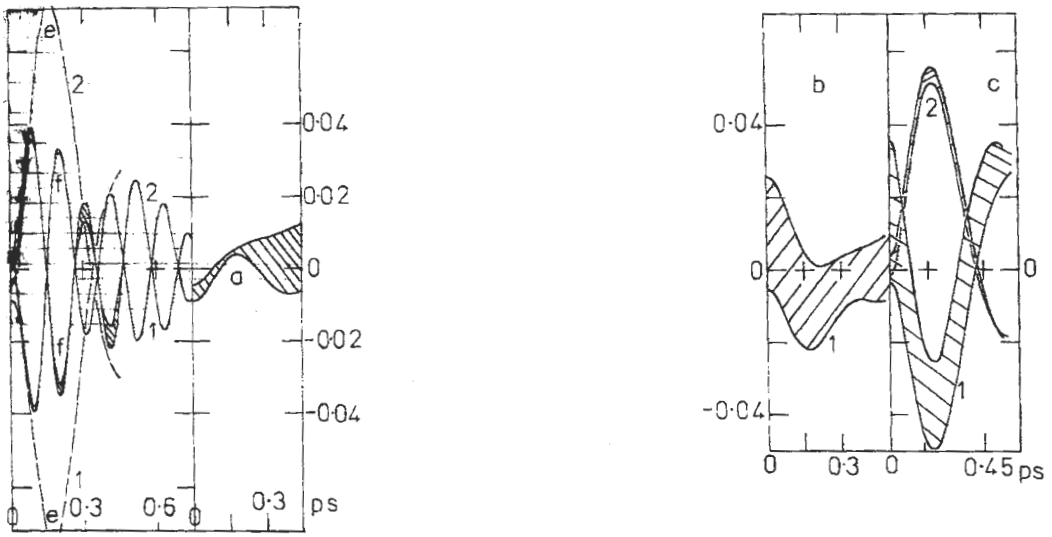

Fig. 1. Development of 1) C_{tr}^{xy} and 2) C_{tr}^{yx} with interaction energy $\mu E/kT$. At $\mu E/kT = 0.0$ the noise level is indicated by the shading. In a noise free simulation this ought to be zero. (a) $\mu E/kT = 0.0$ (noise level); (b) 0.28 (curve 1) only; (c) 1.4; (d) 2.8; (e) 28.0. In this figure the shaded regions indicate the estimated noise level in the computer simulations.
Ordinate: Normalised c.c.f.
Abscissa: time/ps.

have not been able to isolate them satisfactorily from the noise with our simple running-time averaging. A more powerful method for this purpose is "non-equilibrium" or "difference method" computer simulation [18], where the noise is removed precisely, leaving the "signal", i.e. $\mathbf{C}_{tr}$. By analogy, this is also what happens in a dynamic Kerr effect experiment: birefringence is picked up accurately from "well below the thermal noise" (i.e. $\mu E \ll kT$) as the rotation of a polarised probe laser [24]. The technique of induced-birefringence is therefore picking up $\mathbf{C}_{tr}$ in the laboratory frame as a contributory factor in the orientational dynamics. $\mathbf{C}_{tr}$ is therefore directly observable in the laboratory frame with existing techniques. This is discussed theoretically later in this paper.

The dominance of C_{tr}^{xy} and C_{tr}^{yx} can be understood simply in terms of the torque $-\boldsymbol{\mu} \times \mathbf{E}$ when $\mathbf{E}$ is in the z axis. In vector terms this is:

$$(\mathbf{i}\mu_y - \mathbf{j}\mu_x)E_x$$

where $\mathbf{i}$ and $\mathbf{j}$ are unit vectors in the x and y axes and μ_y and μ_x components of the dipole moment $\boldsymbol{\mu}$. The torque is the *same* in overall structure when polarisability effects are introduced,[3] so that little new physical insight is gained in this particular context.

The (x, y) and (y, x) cross-correlation functions are mirror images, and are oscillatory. They attain a maximum normalised amplitude (measured through that of the first peak) for intermediate field strengths. The other elements of $\mathbf{C}_{tr}$ lie below the noise of the current simulation runs. As the field strength is increased the Grigolini decoupling effect is observed in C_{tr}^{xy} and C_{tr}^{yx}. This means that the strong field competes with the thermal forces in the molecular ensemble, whose influence on the correlation function decreases as the field strength increases. In consequence, the c.c.f. becomes longer lived, as measured through the envelope of its oscillations.

At $\mu E/kT = 0.28$ the dominant elements of the c.c.f. $\mathbf{C}_{tr}$ are still just visible above the noise of the simulation (fig. (1)), and it is clear that the computer simulation technique could be used to pick it up for $\mu E/kT \leqq 0.02$ (the condition under which induced birefringence experiments are carried out), given the "difference technique", and long enough runs, to remove the noise. The "difference technique" works, broadly speaking, by picking up the signal from the noise by comparing two simulation runs – one unperturbed and the other slightly perturbed. It illustrates perfectly the fact that $\mathbf{C}_{tr}$ can be picked up directly in the same way by electric-field induced birefringence. The following section deals with the theoretical interpretation of such spectra.

3.1. *Simple Theory of Rototranslation and Birefringence*

Grigolini and co-workers have recently developed [25] a rigorous and general method of solving the Liouville equation of motion for a number of interacting molecules. The basic Liouville equation may be written as:

$$\frac{\mathrm{d}}{\mathrm{d}t}\mathbf{A}(t) = L_0\mathbf{A}(t) \tag{4}$$

where $\mathbf{A}$ is a dynamical stochastic variable, in general a column vector. If we wish to deal with the dynamics of rotation and translation we have:

$$\mathbf{A}(t) = \begin{bmatrix} \mathbf{v}(t) \\ \boldsymbol{\omega}(t) \end{bmatrix} \tag{5}$$

where $\mathbf{v}$ is the centre of mass linear velocity and $\boldsymbol{\omega}$ is the angular velocity of a molecule of the ensemble. Using the methods of modern projection algebra developed by Grigolini et al., eqn. (4) may be rewritten in a form which is closely analogous with the Langevin equation:

$$\frac{\mathrm{d}}{\mathrm{d}t}\mathbf{C}(t) = \boldsymbol{\lambda}(t)\mathbf{C}(t) - \int_0^t \boldsymbol{\varphi}(t-\tau)\mathbf{C}(\tau)\mathrm{d}\tau \tag{6}$$

This is a fundamental equation of motion, rigorous and not phenomenological, for the correlation matrix $\mathbf{C}(t)$ in terms of the matrices $\boldsymbol{\lambda}(t)$ and $\boldsymbol{\varphi}(t-\tau)$, usually known as the "resonance" and "memory" matrices. These may be defined rigorously in terms of equilibrium average involving the dynamical variable $\mathbf{A}$.

For the particular case in which we are interested, it is convenient to define:

$$\mathbf{C}(t) = \begin{bmatrix} \langle \mathbf{v}(t)\mathbf{v}^{\mathrm{T}}(0)\rangle & \langle \mathbf{v}(t)\boldsymbol{\omega}^{\mathrm{T}}(0)\rangle \\ \langle \boldsymbol{\omega}(t)\mathbf{v}^{\mathrm{T}}(0)\rangle & \langle \boldsymbol{\omega}(t)\boldsymbol{\omega}^{\mathrm{T}}(0)\rangle \end{bmatrix}$$

so that the elements of $\mathbf{C}(t)$ are themselves matrices, whose elements in turn are time correlation functions. The evolution of the complete supermatrix $\mathbf{C}(t)$ obeys eqn. (6), the Liouville equation of motion.

In order to reduce the problem at hand to its simplest form, and in order to avoid unnecessary complexity with subsequent loss of clarity, we make the following assumptions.

1) The three molecular moments of inertia are put equal, so that the dynamics of the molecule are those of a "spherical top" with moment of inertia I.

2) It is assumed that the molecule carries a net dipole moment $\boldsymbol{\mu}$, which interacts with an external electric field $\mathbf{E}$. With these assumptions we can define the elements of $\mathbf{C}(t)$ as:

$$\mathbf{C}_{vv} = \langle \mathbf{v}(t)\mathbf{v}^{\mathrm{T}}(0)\rangle = \begin{bmatrix} \langle v_x(t)v_x(0)\rangle & 0 & 0 \\ 0 & \langle v_y(t)v_y(0)\rangle & 0 \\ 0 & 0 & \langle v_z(t)v_z(0)\rangle \end{bmatrix}$$

$$\mathbf{C}_{\omega\omega} = \langle \boldsymbol{\omega}(t)\boldsymbol{\omega}^{\mathrm{T}}(0)\rangle = \begin{bmatrix} \langle \omega_x(t)\omega_x(0)\rangle & 0 & 0 \\ 0 & \langle \omega_y(t)\omega_y(0)\rangle & 0 \\ 0 & 0 & \langle \omega_z(t)\omega_z(0)\rangle \end{bmatrix}$$

$$\mathbf{C}_{v\omega} = \langle \mathbf{v}(t)\boldsymbol{\omega}^{\mathrm{T}}(0)\rangle, (\mathbf{E} \neq \mathbf{0}) = \begin{bmatrix} 0 & \langle v_x(t)\omega_y(0)\rangle & \langle v_x(t)\omega_z(0)\rangle \\ \langle v_y(t)\omega_x(0)\rangle & 0 & \langle v_y(t)\omega_z(0)\rangle \\ \langle v_z(t)\omega_x(0)\rangle & \langle v_z(t)\omega_y(0)\rangle & 0 \end{bmatrix}$$

and similarly for $\mathbf{C}_{\omega v}$.

The sample of molecules is statistically stationary, so that:

$$\mathbf{C}_{\omega v} = \mathbf{C}_{v\omega}$$

Similarly, the matrix of memory functions $\boldsymbol{\varphi}(t)$ is a supermatrix of the form:

$$\boldsymbol{\varphi}(t) = \begin{bmatrix} \boldsymbol{\varphi}_{vv}(t) & \boldsymbol{\varphi}_{v\omega}(t) \\ \boldsymbol{\varphi}_{\omega v}(t) & \boldsymbol{\varphi}_{\omega\omega}(t) \end{bmatrix}$$

For a field $\mathbf{E}$ applied in the z axis of the laboratory frame of reference the computer results have shown that the matrices $\mathbf{C}_{v\omega}(t)$ or $\mathbf{C}_{\omega v}(t)$ may be approximated as

$$\mathbf{C}_{v\omega}(t) = \mathbf{C}_{\omega v}(t) \doteq C^{xy}_{v\omega}(t) \begin{bmatrix} 0 & -1 & 0 \\ 1 & 0 & 0 \\ 0 & 0 & 0 \end{bmatrix} \tag{7}$$

because the dominant elements are the (x,y) and (y,x) elements, which are mirror images. In eqn. (7) $C^{xy}_{v\omega}(t)$ is the scalar c.c.f. element obtained by computer simulation.

It is important to note that the electric field has the dual role of promoting the existence of $C_{v\omega}(t) = C_{\omega v}(t)$ in the laboratory frame and of making the sample *anisotropic*. This means that:

$$\langle v_x^2\rangle = \langle v_y^2\rangle \neq \langle v_z^2\rangle \tag{8}$$

$$\langle \omega_x^2\rangle = \langle \omega_y^2\rangle \neq \langle \omega_z^2\rangle \tag{9}$$

The interaction between $\boldsymbol{\mu}$ and $\mathbf{E}$ appears in eqn. (6) through the matrix $\boldsymbol{\lambda}(t)$. We assume that this matrix can be written in the form:

$$\boldsymbol{\lambda} = i\omega_1 \begin{bmatrix} \mathbf{0} & \mathbf{0} \\ \mathbf{0} & \mathbf{1} \end{bmatrix} \tag{10}$$

where $\mathbf{0}$ is the null matrix and $\mathbf{1}$ the unit matrix, and the scalar frequency

$$\omega_1 = \left(\frac{\mu E_z}{I}\right)^{1/2} \tag{11}$$

Eqn. (10) comes from the fact that the only *direct* influence of $\mathbf{E}$ on the molecular motion is the creation of the *torque* $= \boldsymbol{\mu} \times \mathbf{E}$. There is no *direct* influence on the linear centre of mass velocity ($\mathbf{v}$), so that terms in $\boldsymbol{\lambda}$ involving $\mathbf{v}$ vanish.

Laplace transformation of eqn. (6) gives:

$$[p\mathbf{1} + \boldsymbol{\varphi}(p) - i\omega_1\mathbf{1}]\mathbf{C}(p) = \mathbf{C}(0). \tag{12}$$

The supermatrices in eqn. (12) are defined by:

$$\mathbf{C}(0) = \begin{bmatrix} \mathbf{C}_{vv}(0) & \mathbf{0} \\ \mathbf{0} & \mathbf{C}_{\omega\omega}(0) \end{bmatrix} \tag{13}$$

where:

$$\mathbf{C}_{vv}(0) = \begin{bmatrix} \langle v_x^2\rangle & 0 & 0 \\ 0 & \langle v_y^2\rangle & 0 \\ 0 & 0 & \langle v_z^2\rangle \end{bmatrix}$$

and similarly for $\mathbf{C}_{\omega\omega}(0)$.

$$\mathbf{C}(p) = \begin{bmatrix} \mathbf{C}_{vv}(p) & \mathbf{C}_{v\omega}(p) \\ \mathbf{C}_{\omega v}(p) & \mathbf{C}_{\omega\omega}(p) \end{bmatrix} \tag{14}$$

$$[(p - i\omega_1)\mathbf{1} + \boldsymbol{\varphi}(p)] = \begin{bmatrix} (p - i\omega_1)\mathbf{1} + \boldsymbol{\varphi}_{vv}(p) & \boldsymbol{\varphi}_{v\omega}(p) \\ \boldsymbol{\varphi}_{\omega v}(p) & (p - i\omega_1)\mathbf{1} + \boldsymbol{\varphi}_{\omega\omega}(p) \end{bmatrix} \tag{15}$$

The elements of these matrices are themselves matrices defined by:

$$\boldsymbol{\varphi}_{v\omega} = \boldsymbol{\varphi}_{\omega v} = \boldsymbol{\varphi}^{xy}_{v\omega}(p) \begin{bmatrix} 0 & -1 & 0 \\ 1 & 0 & 0 \\ 0 & 0 & 0 \end{bmatrix}$$

$$\boldsymbol{\varphi}_{vv} = \begin{bmatrix} \phi^{xx}_{vv} & 0 & 0 \\ 0 & \phi^{yy}_{vv} & 0 \\ 0 & 0 & \phi^{zz}_{vv} \end{bmatrix} \quad \text{and so on.}$$

For an electric field $\mathbf{E}$ in the z axis:

$$\begin{aligned} \phi^{xx}_{vv}(p) &= \phi^{yy}_{vv}(p) \neq \phi^{zz}_{vv}(p) \\ \phi^{xx}_{\omega\omega}(p) &= \phi^{yy}_{\omega\omega}(p) \neq \phi^{zz}_{\omega\omega}(p) \end{aligned} \tag{16}$$

and similarly for $C_{vv}(p)$ and $C_{\omega\omega}(p)$ and the linear and angular velocity autocorrelation matrices.

Comparing scalar elements in eqn. (12) provides the following set of scalar equations:

$$C^{xx}_{vv}(p) = [\langle v_x^2\rangle + \phi^{xy}_{v\omega}(p)C^{xy}_{v\omega}(p)]/(p + \phi^{xx}_{vv}(p)) \quad (17)$$

$$= C^{zz}_{vv}(p) = [\langle v_y^2\rangle + \phi^{xy}_{v\omega}(p)C^{xy}_{v\omega}(p)]/(p + \phi^{yy}_{vv}(p)) \quad (18)$$

$$C^{zz}_{vv}(p) = \langle v_z^2\rangle/(p + \phi^{zz}_{vv}(p)) \quad (19)$$

$$C^{xx}_{\omega\omega}(p) = [\langle \omega_x^2\rangle + \phi^{xy}_{v\omega}(p)C^{xy}_{v\omega}(p)]/(p - i\omega_1 + \phi^{xx}_{\omega\omega}(p)) \quad (20)$$

$$= C^{yy}_{\omega\omega}(p) = [\langle \omega_y^2\rangle + \phi^{xy}_{v\omega}(p)C^{xy}_{v\omega}(p)]/(p - i\omega_1 + \phi^{yy}_{\omega\omega}(p)) \quad (21)$$

$$C^{zz}_{\omega\omega}(p) = \langle \omega_z^2\rangle/(p - i\omega_1 + \phi^{zz}_{\omega\omega}(p)) \quad (22)$$

The following physical effects of electric field induced r/t coupling may be deduced from these six equations.

1) For a field E in the z direction both the linear and angular velocity a.c.f.'s become anisotropic in the laboratory frame.

2) For a coupling matrix given by eqn. (7) there is no effect (with this simply theory) of r/t coupling on $C^{zz}_{vv}(p)$ (or $C^{zz}_{vv}(t)$) and $C^{zz}_{\omega\omega}(p)$.

3) The ratios of eqn. (17) to (19) and eqn. (20) to (22) provide the approximate but important result:

$$\phi^{xy}_{v\omega}(p)C^{xy}_{v\omega}(p) \doteq \langle v_z^2\rangle \frac{C^{xx}_{vv}(p)}{C^{zz}_{vv}(p)} - \langle v_x^2\rangle$$

$$\doteq \langle \omega_z^2\rangle \frac{C^{xx}_{\omega\omega}(p)}{C^{zz}_{\omega\omega}(p)} - \langle \omega_x^2\rangle \quad (23)$$

If in the Markov approximation, we regard the memory function as a constant i.e.

$$\phi^{xy}_{v\omega}(p) \doteq \phi^{xy}_{v\omega}$$

then we obtain the following *physical* result:

$$C^{xy}_{v\omega}(p) \doteq \frac{\langle v_z^2\rangle}{\phi^{xy}_{v\omega}} \frac{C^{xx}_{vv}(p)}{C^{zz}_{vv}(p)} - \frac{\langle v_x^2\rangle}{\phi^{xy}_{v\omega}}$$

$$\doteq \frac{\langle \omega_z^2\rangle}{\phi^{xy}_{v\omega}} \frac{C^{xx}_{\omega\omega}(p)}{C^{zz}_{\omega\omega}(p)} - \frac{\langle \omega_x^2\rangle}{\phi^{xy}_{v\omega}} \quad (24)$$

Theorem

Eqn. (24) shows that it is possible to observe the cross-correlation function between linear and angular velocity by applying an electric field to a molecular liquid in the laboratory frame.

In the time domain the cross-correlation function is a convolution of the angular (or linear) autocorrelation function observed in the z direction with the angular or linear autocorrelation function observed in the x or y directions of the laboratory frame (x, y, z), with the electric field applied in the z direction of this frame of reference.

Note that in deriving eqn. (24) we have made the assumptions:

$$\phi^{xx}_{vv}(p) \doteq \phi^{xx}_{vv} \doteq \phi^{zz}_{vv}$$

$$\phi^{xx}_{\omega\omega}(p) \doteq \phi^{xx}_{\omega\omega} \doteq \phi^{zz}_{\omega\omega} \quad (25)$$

If the system (molecular liquid), is quasi-Markovian, and if the birefringence is not very large, eqn. (25) is a good approximation; leading to the physical results summarised in eqn. (24).

4) There are many similar cross-correlations generated by the parity breaking electric field, for which eqn. (24) is a general law, i.e. *all* these new cross-correlation functions are, in principle, observable with the sensitive apparatus used in birefringence experiments (capable of $1:10^6$ accuracy or better).

5) A result specific to our assumption of "spherical top" dynamics can be obtained by eliminating $C^{xx}_{vv}(p)$ between eqns. (17) to (22) and the further four relations:

$$C^{xy}_{v\omega}(p)(p + \phi^{xx}_{vv}(p)) + \phi^{xy}_{v\omega}(p)C^{xx}_{\omega\omega}(p) = 0 \quad (26)$$

$$C^{xy}_{v\omega}(p)(p + \phi^{yy}_{vv}(p)) + \phi^{xy}_{v\omega}(p)C^{yy}_{\omega\omega}(p) = 0 \quad (27)$$

$$C^{xy}_{v\omega}(p)(p - i\omega_1 + \phi^{xx}_{\omega\omega}(p)) + \phi^{xy}_{v\omega}(p)C^{xx}_{vv}(p) = 0 \quad (28)$$

$$C^{xy}_{v\omega}(p)(p - i\omega_1 + \phi^{yy}_{\omega\omega}(p)) + \phi^{xy}_{v\omega}(p)C^{yy}_{\omega\omega}(p) = 0 \quad (29)$$

Eliminating $C^{xx}_{vv}(p)$ between eqns. (17) and (28) and $C^{xx}_{\omega\omega}(p)$ between eqns. (20) and (26) provides the results:

$$\langle v_x^2\rangle = \langle \omega_x^2\rangle$$

$$\langle v_y^2\rangle = \langle \omega_y^2\rangle \quad (30)$$

$$\langle v_z^2\rangle \neq \langle \omega_z^2\rangle$$

This is *not* generally true for "asymmetric top" dynamics, where the Euler terms make the analysis exceedingly complicated without much further physical insight.

Solving simultaneously eqns. (17), (20), (26) and (27) provides a matrix equation with scalar coefficients:

$$\begin{bmatrix} p + \phi^{xx}_{vv}(p) & -\phi^{xy}_{v\omega}(p) \\ \phi^{xy}_{v\omega}(p) & p - i\omega_1 + \phi^{xx}_{\omega\omega}(p) \end{bmatrix} \begin{bmatrix} C^{xx}_{vv}(p) & -C^{xy}_{v\omega}(p) \\ C^{xy}_{v\omega}(p) & C^{xx}_{\omega\omega}(p) \end{bmatrix}$$

$$= \begin{bmatrix} \langle v_x^2\rangle & 0 \\ 0 & \langle \omega_x^2\rangle \end{bmatrix} \quad (31)$$

In order to proceed further without undue complexity we make the Markov approximation and remove the p dependence of $\phi^{xy}_{\omega v}$, ϕ^{xx}_{vv} and $\phi^{xx}_{\omega\omega}$, so that these become constants independent of time. Eqn. (31) then becomes:

$$C^{xx}_{vv}(p) = [\langle v_x^2\rangle(p + \phi^{xx}_{vv})]/D \quad (32)$$

$$C^{xy}_{v\omega}(p) = -\langle \omega_x^2\rangle\phi^{xy}_{v\omega}/D \quad (33)$$

$$C^{xx}_{\omega\omega}(p) = [(p - i\omega_1 + \phi^{xx}_{\omega\omega})\langle \omega_x^2\rangle]/D \quad (34)$$

where:

$$D = (p + \phi^{xx}_{vv})(p - i\omega_1 + \phi^{xx}_{\omega\omega}) + \phi^{xy}_{v\omega}{}^2$$

The cross-correlation function $C^{xy}_{v\omega}(t)$ may now be obtained from the real part of the inverse Laplace transform of eqn. (33), i.e. from the real part of:

$$C^{xy}_{v\omega}(t) = -\frac{\langle \omega_x^2\rangle\phi^{xy}_{v\omega}}{(b - a^2/4)^{1/2}} e^{-at/2} \sin\left[\left(b - \frac{a^2}{4}\right)^{1/2} t\right] \quad (35)$$

where

$$b = \phi^{xy}_{v\omega}{}^2 + \phi^{xx}_{vv}\phi^{xx}_{\omega\omega} - i\omega_1\phi^{xx}_{vv}$$

and

$$a = \phi^{xx}_{vv} + \phi^{xx}_{\omega\omega} - i\omega_1.$$

Note that both the real and imaginary parts of $C^{xy}_{v\omega}(t)$ vanish at $t = 0$, as they should on the grounds that $v_x(0)$ is orthogonal to $\omega_y(0)$. Similarly:

$$C_{vv}^{xx}(t) = \langle\omega_x^2\rangle e^{-at/2}\left[\cos\left[\left(b-\frac{a^2}{4}\right)^{1/2}t\right] + \frac{(\phi_{vv}^{xx}-a/2)}{(b-a^2/4)^{1/2}}\sin\left[\left(b-\frac{a^2}{4}\right)^{1/2}t\right]\right] \quad (36)$$

contains the real and imaginary parts of the linear velocity a.c.f. and

$$C_{\omega\omega}^{xx}(t) = \langle\omega_x^2\rangle e^{-at/2}\left[\cos\left[\left(b-\frac{a^2}{4}\right)^{1/2}t\right] + \frac{(\phi_{\omega\omega}^{xx}-i\omega_1-a/2)}{(b-a^2/4)^{1/2}}\sin\left[\left(b-\frac{a^2}{4}\right)^{1/2}t\right]\right]$$

of the angular velocity a.c.f.

In order to compare eqn. (35), for example, with the computer simulation results we used the identity:

$$\sin(a+ib) = \sin a\cosh b + i\cos a\sinh b \quad (38)$$

and the N.A.G. computer routines A01AAA and A01ACA to evaluate the real part of eqn. (35). The function:

$$\text{Real}\,[C_{v\omega}^{xy}(t)]/\langle\omega_x^2\rangle \quad (39)$$

may then be compared directly with the normalised c.c.f.'s from the computer simulation.

In Figs. (2a) and (2b) we have illustrated function (39) with the test parameters $\phi_{vv}^{xx} = 1.0\times10^{12}\,s^{-1} = \phi_{\omega\omega}^{xx}$. In these curves we have kept the ratio $\omega_1/\phi_{v\omega}^{xy}$ constant. A number of points emerge from the illustration in Figs. (2a) and (2b).

1) The envelope of the oscillations, marked with dashed lines in Figs. (2a) and (2b), remains constant for constant $\omega_1/\phi_{v\omega}^{xy}$.

2) It is possible to observe the function $C_{v\omega}^{xy}$ even for values of $\phi_{v\omega}^{xy}$ much smaller than ϕ_{vv}^{xx} or $\phi_{\omega\omega}^{xx}$.

3) $C_{v\omega}^{xy}(t)$ vanishes, as it should, at $t=0$ and $t\to\infty$. At intermediate t the normalised amplitude of the function is similar to that from the computer. (see Appendix A).

The overall shape of Real $[C_{v\omega}^{xy}(t)]$ in Figs. (2a) and (2b) is similar to that from the computer simulation (fig. (1)) but differs in that the initial slope at $t\to0$ is not zero. Also, for constant $\omega_1/\phi_{v\omega}^{xy}$, the amplitude of Real $[C_{v\omega}^{xy}(t)]/\langle\omega_x^2\rangle$ decreases monotonically with decreasing field strength. (The computer simulated function goes through a maximum at intermediate field strengths.) These are both consequences of the Markov approximation.

The constancy of the oscillation envelope for constant $\omega_1/\phi_{v\omega}^{xy}$ is a useful check on the self-consistency of our calculations for two reasons.

1) The assumption that ϕ_{vv}^{xx}, $\phi_{\omega\omega}^{xx}$ and $\phi_{v\omega}^{xy}$ are independent of time is equivalent to assuming that the correlation functions in the super-matrix $\mathbf{C}(t)$ are Markov in nature. Therefore, for constant $\omega_1/\phi_{v\omega}^{xy}$ there should be no Grigolini decoupling effect, *which is non-Markov in nature.* If there is no Grigolini decoupling effect then the oscillation envelope cannot vary with field strength [19].

2) By parity, $\phi_{v\omega}^{xy}$ must disappear when $\omega_1 = 0$. Therefore, there should be some link between $\phi_{v\omega}^{xy}$ and ω_1. A more complete theory would provide this link in a natural way. The use of constant $\omega_1/\phi_{v\omega}^{xy}$ in Figs. (2a) and (2b) (i.e. $\omega_1 \propto \phi_{v\omega}^{xy}$) produces a constant oscillation envelope for given ϕ_{vv}^{xx} and $\phi_{vv}^{\omega\omega}$ – the result expected from point (1) above. The theory is therefore simple but self-consistent.

4. Conclusions

1) The Liouville equation (4) has been used to produce laboratory frame cross-correlation functions between molecular linear and angular velocity, using a Markov approximation for the memory matrix of eqn. (6), and an applied electric field.

2) Using the indications of computer simulation, summarised in eqn. (7), eqn. (6) leads directly, with some reasonable approximations to eqn. (24).

This equation is an important physical result because it shows that the cross-correlation function $C_{v\omega}^{xy}(t)$ may be observed spectroscopically using electric field-induced birefringence and conventional apparatus. The key result is:

$$C_{v\omega}^{xy}(p) \doteq \frac{\langle\omega_z^2\rangle}{\phi_{v\omega}^{xy}}\frac{C_{\omega\omega}^{xx}(p)}{C_{\omega\omega}^{zz}(p)} - \frac{\langle\omega_x^2\rangle}{\phi_{v\omega}^{xy}} \quad (24)$$

in the Markov approximation.

This shows that $C_{v\omega}^{xy}(t)$, in the time domain, is a *convolution* of $C_{\omega\omega}^{xx}(t)$ and $C_{\omega\omega}^{zz}(t)$, the angular velocity a.c.f.'s in the x and z direction of the laboratory frame. We may reasonably approximate these angular velocity a.c.f.'s with the equivalent *rotational* velocity a.c.f.'s in certain well-known limits, discussed, for example, by Brot [26]. The Fourier transforms of these rotational velocity a.c.f.'s are *far infra-red spectra [12]. Therefore,*

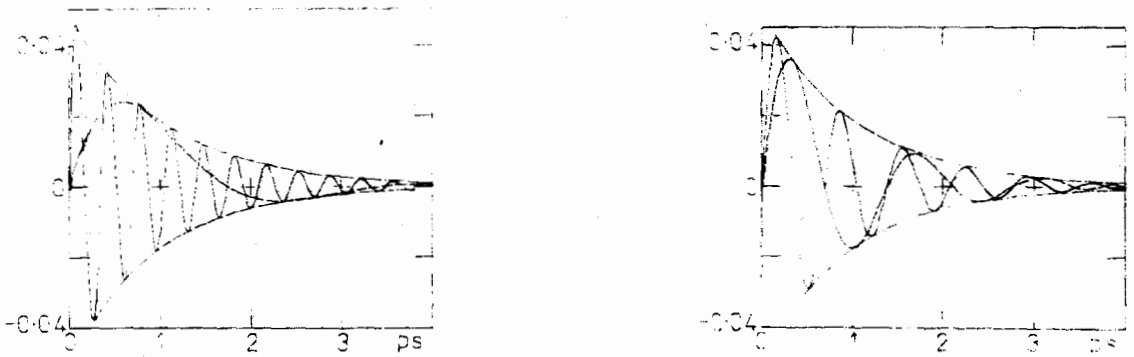

Fig. 2. a) The function $C_{v\omega}^{yx}/\langle\omega_x^2\rangle$ test parameters $\phi_{vv}^{xx} = \phi_{\omega\omega}^{xx} = 10^{12}\,s^{-1}$; ——— $\phi_{v\omega}^{xy} = 0.9\times10^{12}\,s^{-1}$; $\omega_1 = 18.0\times10^{12}\,s^{-1}$; – – – – $\phi_{v\omega}^{xy} = 0.09\times10^{12}\,s^{-1}$; $\omega_1 = 1.8\times10^{12}\,s^{-1}$. ------- The oscillation envelope. b) ——— $\phi_{vv}^{xx} = \phi_{\omega\omega}^{xx} = 10^{12}\,s^{-1}$; $\phi_{v\omega}^{xy} = 0.45\times10^{12}\,s^{-1}$; $\omega_1 = 9.0\times10^{12}\,s^{-1}$; – – – – $\phi_{v\omega}^{xy} = 0.225\times10^{12}\,s^{-1}$; $\omega_1 = 0.45\times10^{12}\,s^{-1}$

Ordinate: $C_{v\omega}^{xy}/\langle\omega_x^2\rangle$ *Abscissa:* time/ps

eqn. (24) shows that ($C^{xy}_{v\omega}(p)$) may be obtained approximately but directly from the ratio of far infra-red spectra of a birefringent liquid. This is an example of, probably, many cross-correlation functions that can be observed in a birefringent medium in this way.

3) *The experimental problem is reduced therefore to simply comparing spectra in different axes of a birefringent liquid.* This task is at its most straightforward in an *aligned dipolar nematic liquid crystal*, which becomes highly birefringent even with weak external electric (or magnetic) fields. It is well known that the *dielectric loss*, for example, is very different in the x and z axes of an aligned dipolar nematic, *and it follows from eqn. (24) that $C^{xy}_{v\omega}$ must, therefore, be of key importance in the dynamics of a liquid crystal.* Future computer simulations will be of great interest in this respect.

Acknowledgements

The University of Wales is thanked for a Fellowship.

References

1. Evans, M. W., Evans, G. J., Coffey, W. T. and Grigolini, P. "Molecular Dynamics", Wiley/Interscience, N.Y., 1982.
2. Coffey, W. T., Evans, M. W. and Grigolini, P. "Molecular Diffusion and Spectra", Wiley/Interscience, N.Y., 1984.
3. Evans, M. W. J. Chem. Phys., **76**, 5473, 5480 (1982); **77**, 4632 (1982); **78**, 925, 5403 (1983).
4. Condiff, D. W. and Dahler, J. S. J. Chem. Phys., **44**, 3988 (1966).
5. Steiger, U. and Fox, R. F. J. Math. Phys., **23**, 296 (1982).
6. Berne, B. J. and Pecora, R. "Dynamic Light Scattering with Reference to Physics, Chemistry and Biology", Wiley/Interscience, N.Y., (1976).
7. Ryckaert, J. P., Bellemans, A. and Ciccotti, G., Mol. Phys., **44** 979 (1981).
8. Evans, M. W. and Ferrario, M. Adv. Mol. Rel. Int. Proc., **22**, 245 (1982).
9. Ferrario, M. and Evans, M. W. Chem. Phys., **23**, 69 (1982).
10. Evans, M. W., Evans, G. J. and Agarwal, V. K. J. Chem. Soc., Faraday Trans II, **79**, 137 (1983).
11. Evans, M. W. and Evans, G. J. ibid., **79**, 153, 767 (1983).
12. Evans, M. W. ibid, **79**, 719, 1331 (1983).
13. Evans, M. W., Baran, J. and Evans, G. J. ibid., **79**, 1473 (1983).
14. Evans, M. W. J. Mol. Liq., **25**, 149 (1983); **26**, 229; **27**, 11 (1983).
15. Evans, M. W. and Evans, G. J. ibid., **25**, 177; **26**, 63 (1983).
16. Evans, M. W. J. Chem. Soc., Chem. Comm., (3), 139 (1983).
17. Evans, M. W. Phys. Rev. Letters, **50**, 371 (1983).
18. Heyes, D. Quart. Rev, CCP5 group, SERC Daresbury Laboratory.
19. Evans, M. W., Grigolini, P. and Marchesoni, F. Chem. Phys. Letters, **95**, 544, 548 (1983).
20. Grigolini, P. Mol. Phys., **30**, 1229 (1975).
21. Morita, A. J. Phys. D, **11**, 1357 (1978); **12(A)**, 991 (1979).
22. Coffey, W. T., Rybarsch, C. and Schroer, W. Phys. Lett., **88A**, 331 (1982).
23. Evans, M. W. Phys. Scripta, **30**, 91 (1984).
24. Elliott, D. A. Ph.D. Thesis, Univ. of Wales, (1982).
25. "Memory Function Approaches to Stochastic Problems in Condensed Matter", special issue in two volumes of "Advances in Chemical Physics", ed. Evans, Grigolini and Pastori, Wiley/Interscience, N.Y., 1984, in press.
26. Brot, C. in "Dielectric and Related Molecular Processes", Vol. 2, p. 1, the Chemical Society, London, 1975, senior reporter M. Davies.

Appendix A

In this appendix we compare the analytical and simulated $C^{xy}_{v\omega}(t)$ and $C^{yx}_{v\omega}(t)$ c.c.f. at 2.8 kT by fitting the simulated $C^{zz}_{\omega\omega}(t)$ function, giving $\phi^{zz}_{\omega\omega} = 6.4$ THz; $\omega_1 = 6.0$ THz. For simplicity, it was then assumed that $\phi^{zz}_{\omega\omega} \doteq \phi^{xx}_{\omega\omega} \doteq \phi^{zz}_{vv} \doteq \phi^{xx}_{vv}$ and the other results were generated by varying $\phi^{xy}_{v\omega}$ only. Figs. (A1) to (A3) are for $\phi^{xy}_{v\omega} = 9.0$ THz. Both the analytical and simulated c.f.'s in Figs. (A1) to (A3) are produced self-

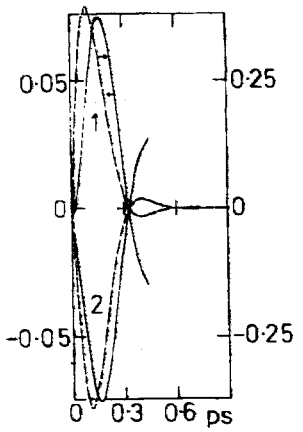

Fig. A(1). Simulated and analytical $C^{xy}_{v\omega}(t)$ and $C^{yx}_{v\omega}(t)$. (1) $C^{xy}_{v\omega}(t)$, simulated; ------ analytical theory (R.H. scale). (2) As for (1), $C^{xy}_{v\omega}(t)$. *Ordinate:* Normalised c.c.f.; *Abscissa:* time/ps

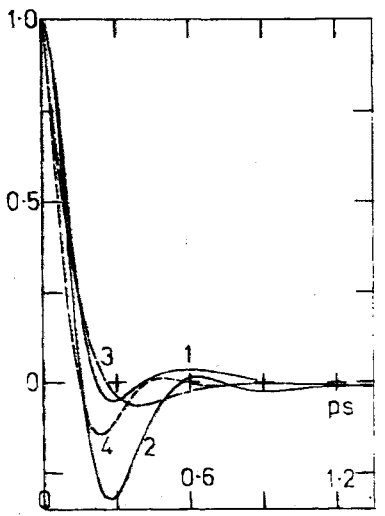

Fig. A(2). (1) $\langle\omega_z(t)\omega_z(0)\rangle/\langle\omega_z^2\rangle$, (2) $\langle\omega_x(t)\omega_x(0)\rangle/\langle\omega_x^2\rangle$ the simulated angular velocity // and ⊥ to the electric field. ------ (3) and (4); As for (1) and (2), respectively, analytical theory.
Ordinate: Normalised c.c.f.; *Abscissa:* time/ps

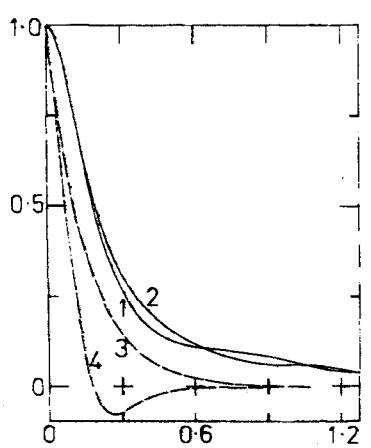

Fig. A(3). As for Fig. (A2); linear, centre of mass, velocity a.c.f.'s.

consistently. For these parameters the analytical c.c.f.'s are greater in normalised intensity than the simulated c.c.f.'s (± 0.35 c.f. ± 0.07), and less oscillatory (because of the Markov structure of ϕ). The birefringence in the simulated and analytical angular velocity a.c.f.'s in the same sense (Fig. (A2).), but this time the analytical result is the smaller in magnitude. In Fig. (A3) there is a small (but real) birefringence in the simulated linear velocity a.c.f. which, as $t \to \infty$, is in the same sense but much smaller, this time, than the Markov analytical result.

Overall, therefore, both theory and simulation point clearly towards the way to measure $C^{xy}_{\dot{\mu}\omega}(t)$ and $C^{yx}_{\dot{\mu}\omega}(t)$. We note to finish that: i) the analytical theory used here is the simplest possible (with no time dependence for ϕ), and can be improved with the methods of Grigolini et al.[25] ii) An entirely analogous theory could be constructed for $\langle \mathbf{v}(t)\dot{\boldsymbol{\mu}}^{\mathrm{T}}(0)\rangle$. By computer simulation, the dominant element is $\langle v_x(t)\dot{\mu}_x(0)\rangle$. In consequence, the birefringence in $\langle \dot{\boldsymbol{\mu}}(t)\cdot\dot{\boldsymbol{\mu}}(0)\rangle$ is opposite in sense to that in $\langle \boldsymbol{\omega}(t)\cdot\boldsymbol{\omega}(0)\rangle$ for the same z axis electric field. This could be picked up directly and accurately using polarized probe carcinotrons as far infra-red birefringence at different spot frequencies.